16

Measurement and Characterization of Solar Cells and Modules

Keith Emery

National Renewable Energy Laboratory, Golden, CO, USA

16.1 INTRODUCTION

Methods of assessing the performance of photovoltaic cells and modules are described in this chapter. The performance of cells and modules can be described by their current versus voltage ($I-V$) and spectral responsivity versus wavelength ($S(\lambda)$) characteristics. Measurement equipment, procedures, and artifacts are discussed for $I-V$ and $S(\lambda)$. The most common performance indicator is the photovoltaic (PV) efficiency under standard reporting conditions (SRC) (temperature, spectral irradiance, total irradiance). The efficiency is the maximum electrical power divided by the total irradiance. Procedures for accurately determining the efficiency or the maximum power with respect to reference conditions are described. Alternatives to the standard peak watt rating and how they compare with actual field performance are discussed. Since photovoltaics must operate for 20 to 30 years, with a degradation of less than 1% per year, procedures for assessing the durability of PV modules are also discussed.

16.2 RATING PV PERFORMANCE

A variety of performance indicators have been employed by the photovoltaic community to rate the performance of PV cells and modules [1–4]. Domestic and international consensus standards have been adopted to rate the performance of PV cells and modules in terms of the output power, or equivalently their efficiency with respect to SRC defined by temperature, spectral irradiance, and total irradiance [5–15]. Modules and systems are rated by their peak power under SRC because manufacturers sell and customers purchase PV modules and systems according to the price per watt of power produced. Other performance indicators may be more appropriate for niche markets, such as aesthetics

Handbook of Photovoltaic Science and Engineering. Edited by A. Luque and S. Hegedus
ISBN: 0-471-49196-9

for building-integrated photovoltaics, liters per day for water pumping, or low light-level operation for consumer electronics [4].

The actual output of a PV module or system in the field is a function of orientation, total irradiance, spectral irradiance, wind speed, air temperature, soiling, and various system-related losses. Various module- and system-rating methods attempt to ensure that the actual performance is comparable to the rated performance to keep the resulting level of customer satisfaction high.

16.2.1 Standard Reporting Conditions

The PV performance in terms of SRC is commonly expressed in terms of efficiency. At the research level, an internationally accepted set of SRC is essential to prevent the researcher from adjusting the reporting conditions to maximize the efficiency. The procedures for measuring the performance with respect to SRC must be quick, easy, reproducible, and accurate for the research cell fresh out of the deposition system or for the module on a factory floor with production goals. The PV conversion efficiency (η) is calculated from the measured maximum or peak PV power (P_{max}), device area (A), and total incident irradiance (E_{tot}):

$$\eta = \frac{P_{\text{max}}}{E_{\text{tot}} A} 100 \tag{16.1}$$

The term *reporting*, rather than *reference* or *test*, is used because a measurement can be performed at conditions other than SRC and then carefully corrected to be equivalent to being measured at SRC. The SRC for rating the performance of cells and modules are summarized in Table 16.1 [1, 5–15]. The direct, global, and AM0 reference spectra are summarized in Figure 16.1 and Tables 16.2 and 16.3.

As a matter of shorthand, the global and direct terrestrial reference spectra are often referred to as AM1.5 G and AM1.5 D, respectively. Many groups often just refer to the reference spectrum as AM1.5. This can be confusing without a reference because numerous different AM1.5 reference spectra have been proposed and used in the past. It should be noted that neither the direct reference spectrum nor the global reference spectrum actually integrates to exactly 1000 Wm^{-2} [10, 12, 13, 17]. The global reference spectrum integrates to approximately 963 Wm^{-2} and the direct reference spectrum

Table 16.1 Standard reference conditions for rating photovoltaic cells, modules and systems

Application	Irradiance [Wm^{-2}]	Reference Spectrum	Temperature [°C]
Terrestrial			
Cells	1000	Global [5]	25 cell [5, 6, 11]
Modules, systems	1000	Global [11, 13]	25 cell [7] or NOCT [7]
Modules, systems	1000[a]	Prevailing	20 ambient
Concentration[b]	>1000	Direct [10]	25 cell [5]
Extraterrestrial[c]	1366 [8], 1367 [14]	AM0 [8, 14, 15]	25 [15], 28 cell [16]

[a] Linear regression of power to project test conditions, 850 Wm^{-2} with a 5° field of view for concentrator systems
[b] At present, no consensus standards exist although ASTM and the European Community are developing standards
[c] At present no consensus standards exist although there is an ISO draft standard [15]

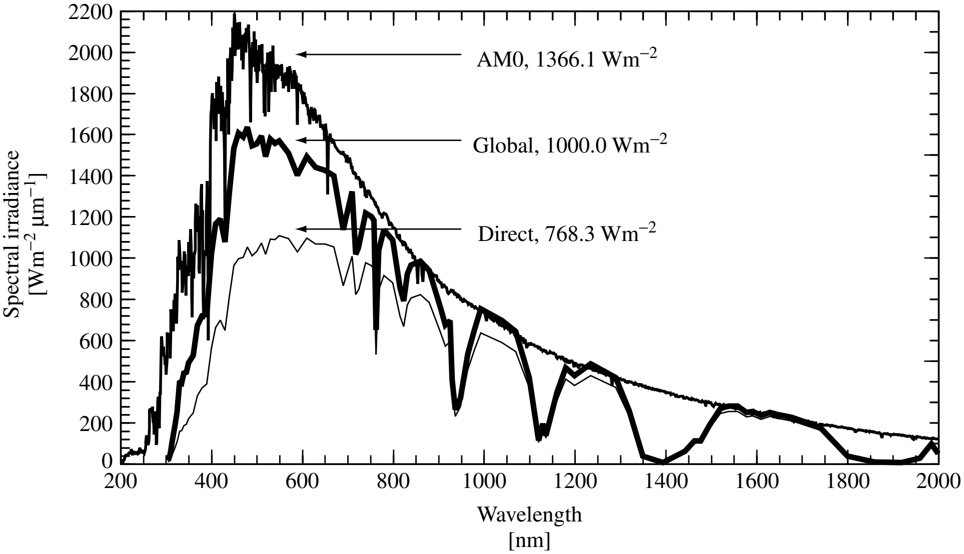

Figure 16.1 Global, Direct, and AM0 reference spectra listed in Tables 16.2 and 16.3. Adapted with permission from the Annual Book of ASTM Standards, Copyright ASTM [10, 12, 13]

integrates to approximately 768 Wm^{-2}. Different numerical integration methods give differences in the integrated or total irradiance of the reference spectra at the 0.1% level because of the relatively small number of data points (120) and the large variations in the spectral irradiance with wavelength. The structure in the spectral irradiance is a function of bandwidth. The bandwidth in the spectral irradiance at any given wavelength is approximately the difference in wavelength between adjacent points. The PV community has arbitrarily taken the term "one sun" to mean a total irradiance of 1000 Wm^{-2} [17]. In fact, the spectral irradiance of the global reference spectrum normalized to 1000 Wm^{-2} in Table 16.2 and Figure 16.1 exceeds the AM0 spectral irradiance in the infrared, which is not physically possible without concentration. The term *global* in Tables 16.1 and 16.2 refers to the spectral irradiance distribution on a 37° tilted south-facing surface with a solar zenith angle of 48.19° (AM1.5). The term *direct* in Tables 16.1 and 16.2 refers to the direct-normal component (5° field of view) of the global spectral irradiance distribution [18]. The term AM1 or AM1.5 is often used to refer to standard spectra, but the relative optical air mass (AM) is a geometrical quantity and can be obtained by taking the secant of the zenith angle (See Section 20.3 for a more complete explanation of AM.). For AM1, the zenith angle is 0°. The relative optical air mass can be pressure-corrected to an absolute air mass by multiplying by the barometric pressure and dividing by the sea level pressure. In outer space the pressure is zero so the absolute air mass is always zero. The internationally accepted global reference spectrum is based upon the 1962 US standard atmosphere with a rural aerosol distribution as input to a sophisticated Monte Carlo ray-tracing model for wavelengths up to 2500 nm and an undocumented simple direct-normal spectral model for the irradiances from 2500 nm to 4050 nm [12, 13, 18]. The fact that the reference spectrum only approximates the "real-world" spectra at solar noon is unimportant as long as the differences between the photocurrents are the same for various PV

Table 16.2 Standard direct and global reference spectra adapted with permission from the annual book of ASTM standards, Copyright ASTM [10, 11]. The global spectrum integrates to 1000.0 Wm^{-2} and the direct spectrum integrates to 768.3 Wm^{-2}

Wavelength [nm]	Global $[\mathrm{Wm}^{-2}\ \mu\mathrm{m}^{-1}]$	Direct $[\mathrm{Wm}^{-2}\ \mu\mathrm{m}^{-1}]$	Wavelength [nm]	Global $[\mathrm{Wm}^{-2}\ \mu\mathrm{m}^{-1}]$	Direct $[\mathrm{Wm}^{-2}\ \mu\mathrm{m}^{-1}]$	Wavelength [nm]	Global $[\mathrm{Wm}^{-2}\ \mu\mathrm{m}^{-1}]$	Direct $[\mathrm{Wm}^{-2}\ \mu\mathrm{m}^{-1}]$
–	–	–	–	–	–	–	–	–
305	9.5	3.4	740	1211.2	971.0	1520	262.6	239.3
310	42.3	15.6	753	1193.9	956.3	1539	274.2	248.8
315	107.8	41.1	758	1175.5	942.2	1558	275.0	249.3
320	181.0	71.2	763	643.1	524.8	1578	244.6	222.3
325	246.8	100.2	768	1030.7	830.7	1592	247.4	227.3
330	395.3	152.4	780	1131.1	908.9	1610	228.7	210.5
335	390.1	155.6	800	1081.6	873.4	1630	244.5	224.7
340	435.3	179.4	816	849.2	712.0	1646	234.8	215.9
345	438.9	186.7	824	785.0	660.2	1678	220.5	202.8
350	483.7	212.0	832	916.4	765.5	1740	171.5	158.2
360	520.3	240.5	840	959.9	799.8	1800	30.7	28.6
370	666.2	324.0	860	978.9	815.2	1860	2.0	1.8
380	712.5	362.4	880	933.2	778.3	1920	1.2	1.1
390	720.7	381.7	905	748.5	630.4	1960	21.2	19.7
400	1013.1	556.0	915	667.5	565.2	1985	91.1	84.9
410	1158.2	656.3	925	690.3	586.4	2005	26.8	25.0
420	1184.0	690.8	930	403.6	348.1	2035	99.5	92.5
430	1071.9	641.9	937	258.3	224.2	2065	60.4	56.3
440	1302.0	798.5	948	313.6	271.4	2100	89.1	82.7
450	1526.0	956.6	965	526.8	451.2	2148	82.2	76.2
460	1599.6	990.8	980	646.4	549.7	2198	71.5	66.4
470	1581.0	998.0	993	746.8	630.1	2270	70.2	65.0
480	1628.3	1046.1	1040	690.5	582.9	2360	62.0	57.6
490	1539.2	1005.1	1070	637.5	539.7	2450	21.2	19.8
500	1548.7	1026.7	1100	412.6	366.2	2494	18.5	17.0
510	1586.5	1066.7	1120	108.9	98.1	2537	3.2	3.0
520	1484.9	1011.5	1130	189.1	169.5	2941	4.4	4.0
530	1572.4	1084.9	1137	132.2	118.7	2973	7.6	7.0
540	1550.7	1082.4	1161	339.0	301.9	3005	6.5	6.0
550	1561.5	1102.2	1180	460.0	406.8	3056	3.2	3.0
570	1501.5	1087.4	1200	423.6	375.2	3132	5.4	5.0
590	1395.5	1024.3	1235	480.5	423.6	3156	19.4	18.0
610	1485.3	1088.8	1290	413.1	365.7	3204	1.3	1.2
630	1434.1	1062.1	1320	250.2	223.4	3245	3.2	3.0
650	1419.9	1061.7	1350	32.5	30.1	3317	13.1	12.0
670	1392.3	1046.2	1395	1.6	1.4	3344	3.2	3.0
690	1130.0	859.2	1443	55.7	51.6	3450	13.3	12.2
710	1316.7	1002.4	1463	105.1	97.0	3573	11.9	11.0
718	1010.3	816.9	1477	105.5	97.3	3765	9.8	9.0
724	1043.2	842.8	1497	182.1	167.1	4045	7.5	6.9

Table 16.3 AM0 standard solar spectrum adapted with permission from the annual book of ASTM standards, Copyright ASTM [8]

λ [nm]	$E(\lambda)$ [Wm^{-2} μm^{-1}]	λ [nm]	$E(\lambda)$ [Wm^{-2} μm^{-1}]	λ [nm]	$E(\lambda)$ [Wm^{-2} μm^{-1}]	λ [nm]	$E(\lambda)$ [Wm^{-2} μm^{-1}]	λ [nm]	$E(\lambda)$ [Wm^{-2} μm^{-1}]	λ [nm]	$E(\lambda)$ [Wm^{-2} μm^{-1}]	λ [nm]	$E(\lambda)$ [Wm^{-2} μm^{-1}]	λ [nm]	$E(\lambda)$ [Wm^{-2} μm^{-1}]	λ [nm]	$E(\lambda)$ [Wm^{-2} μm^{-1}]
–	–	–	–	–	–	–	–	–	–	–	–	–	–	–	–	–	–
119.5	6.30E − 2	320.5	820.6	521.5	1939	719.8	1388.0	1088	577.8	1490	296.2	1892	137.0	2294	67.99	4460	5.799
120.5	5.72E − 1	321.5	713	522.5	1855	720.7	1385.0	1090	599.3	1492	294.1	1894	135.3	2296	68.52	4480	5.694
121.5	5.00E + 0	322.5	701.8	523.5	1927	721.7	1386.0	1092	592.8	1494	296.2	1896	132.5	2298	68.39	4500	5.591
122.5	1.21E + 0	323.5	674	524.5	1992	722.7	1383.0	1094	555.9	1496	287.2	1898	137.1	2300	68.75	4520	5.491
123.5	4.86E − 2	324.5	775.4	525.5	1963	723.6	1389.0	1096	570.7	1498	291.2	1900	136.0	2302	68.89	4540	5.392
124.5	3.50E − 2	325.5	892.6	526.5	1702	724.6	1384.0	1098	569.5	1500	290.7	1902	138.9	2304	68.78	4560	5.296
125.5	2.94E − 2	326.5	998.3	527.5	1860	725.5	1372.0	1100	583.2	1502	278.9	1904	135.9	2306	68.64	4580	5.202
126.5	3.59E − 2	327.5	971	528.5	1930	726.5	1375.0	1102	570.4	1504	274.6	1906	136.5	2308	68.48	4600	5.110
127.5	2.17E − 2	328.5	935.2	529.5	1951	727.4	1374.0	1104	576.9	1506	271.9	1908	135.3	2310	68.08	4620	5.020
128.5	1.76E − 2	329.5	1081	530.5	1986	728.4	1347.0	1106	576.0	1508	281.1	1910	136.2	2312	68.00	4640	4.932
129.5	4.07E − 2	330.5	1036	531.5	1997	729.3	1332.0	1108	573.2	1510	288.8	1912	133.0	2314	67.98	4660	4.846
130.5	1.23E − 1	331.5	984.2	532.5	1801	730.3	1364.0	1110	573.0	1512	283.3	1914	135.5	2316	67.05	4680	4.762
131.5	4.06E − 2	332.5	973.2	533.5	1956	731.2	1358.0	1112	564.6	1514	281.1	1916	134.2	2318	66.42	4700	4.680
132.5	4.21E − 2	333.5	939.3	534.5	1890	732.2	1360.0	1114	565.3	1516	282.5	1918	133.5	2320	67.15	4720	4.599
133.5	1.71E − 1	334.5	977.3	535.5	2024	733.1	1351.0	1116	565.9	1518	283.3	1920	131.1	2322	65.70	4740	4.520
134.5	4.66E − 2	335.5	961.4	536.5	1903	734.0	1364.0	1118	563.6	1520	282.2	1922	133.5	2324	64.33	4760	4.443
135.5	3.88E − 2	336.5	825	537.5	1914	735.0	1348.0	1120	552.0	1522	274.6	1924	131.4	2326	64.30	4780	4.367
136.5	3.15E − 2	337.5	858	538.5	1937	735.9	1335.0	1122	561.0	1524	276.6	1926	132.3	2328	65.51	4800	4.293
137.5	2.98E − 2	338.5	939.2	539.5	1864	736.9	1337.0	1124	557.6	1526	280.5	1928	128.8	2330	65.65	4820	4.221
138.5	4.04E − 2	339.5	976.5	540.5	1800	737.8	1333.0	1126	543.3	1528	281.0	1930	128.5	2332	64.89	4840	4.150
139.5	7.71E − 2	340.5	1026	541.5	1913	738.8	1292.0	1128	550.8	1530	269.3	1932	126.8	2334	65.23	4860	4.080
140.5	6.19E − 2	341.5	941.5	542.5	1857	739.7	1309.0	1130	542.6	1532	278.0	1934	128.8	2336	64.33	4880	4.012
141.5	4.29E − 2	342.5	1012	543.5	1911	740.7	1295.0	1132	545.9	1534	272.8	1936	128.5	2338	64.06	4900	3.946
142.5	4.77E − 2	343.5	968.8	544.5	1911	741.6	1286.0	1134	542.1	1536	276.5	1938	128.9	2340	64.87	4920	3.881
143.5	5.21E − 2	344.5	810.9	545.5	1934	742.6	1307.0	1136	546.0	1538	273.3	1940	124.5	2342	64.77	4940	3.817

(*continued overleaf*)

Table 16.3 *(continued)*

λ [nm]	$E(\lambda)$ [Wm^{-2} $\mu\mathrm{m}^{-1}$]	λ [nm]	$E(\lambda)$ [Wm^{-2} $\mu\mathrm{m}^{-1}$]	λ [nm]	$E(\lambda)$ [Wm^{-2} $\mu\mathrm{m}^{-1}$]	λ [nm]	$E(\lambda)$ [Wm^{-2} $\mu\mathrm{m}^{-1}$]	λ [nm]	$E(\lambda)$ [Wm^{-2} $\mu\mathrm{m}^{-1}$]	λ [nm]	$E(\lambda)$ [Wm^{-2} $\mu\mathrm{m}^{-1}$]	λ [nm]	$E(\lambda)$ [Wm^{-2} $\mu\mathrm{m}^{-1}$]	λ [nm]	$E(\lambda)$ [Wm^{-2} $\mu\mathrm{m}^{-1}$]	λ [nm]	$E(\lambda)$ [Wm^{-2} $\mu\mathrm{m}^{-1}$]
144.5	5.19E − 2	345.5	957.2	546.5	1911	743.5	1324.0	1138	534.1	1540	267.8	1942	126.0	2344	64.61	4960	3.754
145.5	5.64E − 2	346.5	944.1	547.5	1865	744.4	1309.0	1140	529.4	1542	270.3	1944	115.2	2346	64.23	4980	3.693
146.5	7.22E − 2	347.5	919	548.5	1895	745.4	1324.0	1142	531.8	1544	274.2	1946	113.6	2348	64.24	5000	3.633
147.5	8.65E − 2	348.5	914.4	549.5	1928	746.3	1316.0	1144	531.1	1546	273.6	1948	123.7	2350	64.13	5050	3.519
148.5	8.36E − 2	349.5	906.9	550.5	1894	747.3	1322.0	1146	538.2	1548	266.0	1950	123.5	2352	61.50	5100	3.387
149.5	8.11E − 2	350.5	1070	551.5	1903	748.2	1320.0	1148	533.9	1550	265.4	1952	119.8	2354	61.29	5150	3.261
150.5	8.86E − 2	351.5	998.3	552.5	1878	749.2	1297.0	1150	532.2	1552	268.9	1954	125.8	2356	62.34	5200	3.142
151.5	9.44E − 2	352.5	925.3	553.5	1914	750.1	1299.0	1152	529.2	1554	260.5	1956	125.0	2358	61.44	5250	3.028
152.5	1.19E − 1	353.5	1052	554.5	1931	752.0	1285.0	1154	531.3	1556	262.7	1958	124.7	2360	62.23	5300	2.919
153.5	1.32E − 1	354.5	1132	555.5	1930	754.0	1285.0	1156	526.4	1558	263.7	1960	123.7	2362	62.47	5350	2.814
154.5	2.10E − 1	355.5	1065	556.5	1853	756.0	1280.0	1158	525.4	1560	262.8	1962	122.6	2364	62.16	5400	2.715
155.5	2.19E − 1	356.5	929.8	557.5	1878	758.0	1271.0	1160	513.6	1562	264.5	1964	118.8	2366	62.07	5450	2.620
156.5	1.88E − 1	357.5	811.3	558.5	1818	760.0	1257.0	1162	506.8	1564	261.4	1966	120.7	2368	61.96	5500	2.529
157.5	1.75E − 1	358.5	706.9	559.5	1839	762.0	1260.0	1164	512.0	1566	257.5	1968	122.9	2370	61.18	5550	2.442
158.5	1.71E − 1	359.5	1010	560.5	1875	764.0	1243.0	1166	511.9	1568	256.2	1970	121.7	2372	61.47	5600	2.358
159.5	1.79E − 1	360.5	989.4	561.5	1856	766.0	1239.0	1168	513.9	1570	257.5	1972	117.9	2374	59.19	5650	2.279
160.5	1.97E − 1	361.5	895	562.5	1882	768.0	1224.0	1170	505.4	1572	258.9	1974	119.8	2376	61.03	5700	2.202
161.5	2.27E − 1	362.5	1017	563.5	1893	770.0	1215.0	1172	512.5	1574	253.4	1976	120.6	2378	61.37	5750	2.129
162.5	2.57E − 1	363.5	1016	564.5	1886	772.0	1206.0	1174	511.8	1576	244.7	1978	116.9	2380	61.05	5800	2.059
163.5	2.90E − 1	364.5	1033	565.5	1829	774.0	1205.0	1176	497.6	1578	241.6	1980	117.9	2382	60.29	5850	1.992
164.5	3.03E − 1	365.5	1174	566.5	1861	776.0	1186.0	1178	494.6	1580	256.2	1982	118.0	2384	57.17	5900	1.927
165.5	4.39E − 1	366.5	1256	567.5	1920	778.0	1207.0	1180	506.7	1582	246.8	1984	117.9	2386	57.25	5950	1.865
166.5	4.07E − 1	367.5	1203	568.5	1841	780.0	1212.0	1182	499.5	1584	250.2	1986	114.4	2388	59.29	6000	1.806
167.5	3.95E − 1	368.5	1122	569.5	1892	782.0	1206.0	1184	482.7	1586	251.0	1988	118.6	2390	59.41	6050	1.749
168.5	4.64E − 1	369.5	1249	570.5	1800	784.0	1207.0	1186	497.8	1588	240.0	1990	118.2	2392	59.09	6100	1.694
169.5	5.99E − 1	370.5	1161	571.5	1855	786.0	1202.0	1188	481.0	1590	228.5	1992	116.4	2394	59.10	6150	1.641
170.5	6.74E − 1	371.5	1197	572.5	1925	788.0	1191.0	1190	490.3	1592	243.6	1994	114.1	2396	58.90	6200	1.591

171.5	7.01E − 1	372.5	1074	573.5	1908	790.0	1174.0	1192	494.5	1594	251.3	1996	115.7	2398	59.22	6250	1.542
172.5	7.39E − 1	373.5	937.8	574.5	1899	792.0	1149.0	1194	493.7	1596	241.0	1998	114.5	2400	58.33	6300	1.495
173.5	7.79E − 1	374.5	917.6	575.5	1862	794.0	1166.0	1196	486.2	1598	250.9	2000	115.9	2402	58.82	6350	1.450
174.5	9.24E − 1	375.5	1082	576.5	1878	796.0	1161.0	1198	464.1	1600	243.5	2002	114.6	2404	58.60	6400	1.407
175.5	1.10E + 0	376.5	1106	577.5	1889	798.0	1152.0	1200	476.9	1602	243.9	2004	113.7	2406	58.32	6450	1.365
176.5	1.24E + 0	377.5	1306	578.5	1814	800.0	1143.0	1202	486.2	1604	243.5	2006	113.4	2408	58.21	6500	1.325
177.5	1.43E + 0	378.5	1353	579.5	1860	802.0	1139.0	1204	466.6	1606	242.1	2008	114.5	2410	58.13	6550	1.286
178.5	1.57E + 0	379.5	1087	580.5	1870	804.0	1137.0	1206	480.8	1608	244.3	2010	113.9	2412	58.09	6600	1.249
179.5	1.61E + 0	380.5	1225	581.5	1885	806.0	1130.0	1208	458.7	1610	232.5	2012	113.4	2414	55.61	6650	1.213
180.5	1.87E + 0	381.5	1103	582.5	1905	808.0	1110.0	1210	468.9	1612	237.9	2014	112.5	2416	54.02	6700	1.178
181.5	2.28E + 0	382.5	806.5	583.5	1889	810.0	1095.0	1212	474.0	1614	240.5	2016	112.7	2418	56.76	6750	1.145
182.5	2.29E + 0	383.5	697.2	584.5	1892	812.0	1091.0	1214	474.8	1616	228.9	2018	112.3	2420	56.40	6800	1.112
183.5	2.29E + 0	384.5	978.1	585.5	1814	814.0	1110.0	1216	474.7	1618	240.2	2020	110.7	2422	56.59	6850	1.081
184.5	2.11E + 0	385.5	1028	586.5	1862	816.0	1080.0	1218	471.7	1620	230.9	2022	108.6	2424	56.16	6900	1.051
185.5	2.36E + 0	386.5	1026	587.5	1880	818.0	1076.0	1220	469.4	1622	235.6	2024	110.3	2426	56.11	6950	1.022
186.5	2.75E + 0	387.5	1023	588.5	1780	820.0	1069.0	1222	468.0	1624	238.6	2026	110.3	2428	56.05	7000	0.994
187.5	3.07E + 0	388.5	1003	589.5	1640	822.0	1053.0	1224	465.6	1626	237.7	2028	109.4	2430	56.28	7050	0.967
188.5	3.35E + 0	389.5	1196	590.5	1844	824.0	1072.0	1226	464.8	1628	239.7	2030	106.8	2432	55.96	7100	0.941
189.5	3.64E + 0	390.5	1271	591.5	1818	826.0	1068.0	1228	457.4	1630	235.9	2032	109.4	2434	55.49	7150	0.916
190.5	3.84E + 0	391.5	1367	592.5	1839	828.0	1060.0	1230	461.5	1632	234.7	2034	107.7	2436	54.93	7200	0.892
191.5	4.25E + 0	392.5	1039	593.5	1827	830.0	1033.0	1232	457.9	1634	231.9	2036	107.6	2438	54.89	7250	0.868
192.5	4.19E + 0	393.5	593.4	594.5	1804	832.0	1047.0	1234	457.2	1636	229.0	2038	104.7	2440	55.47	7300	0.845
193.5	3.88E + 0	394.5	1046	595.5	1813	834.0	1028.0	1236	456.4	1638	222.4	2040	107.7	2442	55.25	7350	0.823
194.5	5.31E + 0	395.5	1339	596.5	1836	836.0	1019.0	1238	456.5	1640	221.6	2042	106.9	2444	55.10	7400	0.802
195.5	5.53E + 0	396.5	870.9	597.5	1811	838.0	1038.0	1240	449.7	1642	221.1	2044	107.2	2446	53.86	7450	0.781
196.5	6.12E + 0	397.5	946.6	598.5	1788	840.0	1017.0	1242	448.5	1644	220.7	2046	106.9	2448	53.35	7500	0.761
197.5	6.31E + 0	398.5	1552	599.5	1805	842.0	1020.0	1244	446.4	1646	226.6	2048	105.9	2450	53.20	7550	0.742
198.5	6.31E + 0	399.5	1695	600.1	1786	844.0	990.7	1246	447.5	1648	226.9	2050	105.8	2452	53.13	7600	0.723
199.5	6.79E + 0	400.5	1714	601.1	1762	846.0	1001.0	1248	446.6	1650	222.3	2052	104.3	2454	53.73	7650	0.705

(*continued overleaf*)

Table 16.3 (*continued*)

λ [nm]	$E(\lambda)$ [Wm^{-2} μm^{-1}]	λ [nm]	$E(\lambda)$ [Wm^{-2} μm^{-1}]	λ [nm]	$E(\lambda)$ [Wm^{-2} μm^{-1}]	λ [nm]	$E(\lambda)$ [Wm^{-2} μm^{-1}]	λ [nm]	$E(\lambda)$ [Wm^{-2} μm^{-1}]	λ [nm]	$E(\lambda)$ [Wm^{-2} μm^{-1}]	λ [nm]	$E(\lambda)$ [Wm^{-2} μm^{-1}]	λ [nm]	$E(\lambda)$ [Wm^{-2} μm^{-1}]	λ [nm]	$E(\lambda)$ [Wm^{-2} μm^{-1}]
200.5	7.47E + 0	401.5	1780	602.1	1740	848.0	1003.0	1250	446.5	1652	222.8	2054	104.7	2456	52.76	7700	0.688
201.5	8.18E + 0	402.5	1793	603.1	1784	850.0	967.0	1252	439.6	1654	224.8	2056	104.7	2458	52.11	7750	0.671
202.5	8.42E + 0	403.5	1716	604.1	1797	852.0	957.1	1254	441.3	1656	224.5	2058	104.0	2460	53.62	7800	0.654
203.5	9.39E + 0	404.5	1706	605.1	1791	854.0	867.9	1256	438.4	1658	224.3	2060	102.0	2462	53.43	7850	0.638
204.5	10.450	405.5	1699	606.1	1772	856.0	939.2	1258	436.8	1660	221.9	2062	103.9	2464	53.40	7900	0.623
205.5	10.740	406.5	1619	607.1	1776	858.0	984.8	1260	436.9	1662	222.6	2064	99.7	2466	53.12	7950	0.608
206.5	11.290	407.5	1659	608.0	1751	860.0	959.0	1262	433.6	1664	221.1	2066	103.1	2468	53.06	8000	0.593
207.5	12.900	408.5	1768	609.0	1740	862.0	975.9	1264	432.2	1666	217.7	2068	102.3	2470	51.39	8050	0.579
208.5	15.340	409.5	1747	610.0	1728	864.0	912.5	1266	430.7	1668	214.5	2070	100.3	2472	52.84	8100	0.565
209.5	21.790	410.5	1561	611.0	1740	866.0	878.8	1268	424.0	1670	219.8	2072	101.2	2474	51.77	8150	0.552
210.5	28.450	411.5	1849	612.0	1730	868.0	953.1	1270	430.4	1672	210.8	2074	101.7	2476	52.51	8200	0.539
211.5	34.180	412.5	1820	613.0	1720	870.0	951.1	1272	428.7	1674	215.6	2076	101.3	2478	52.12	8250	0.527
212.5	31.900	413.5	1786	614.0	1685	872.0	944.2	1274	424.5	1676	208.5	2078	101.0	2480	49.95	8300	0.514
213.5	33.790	414.5	1766	615.0	1712	874.0	947.1	1276	426.0	1678	211.7	2080	98.7	2482	49.96	8350	0.503
214.5	40.800	415.5	1763	616.0	1661	876.0	949.1	1278	423.6	1680	202.0	2082	99.9	2484	51.60	8400	0.491
215.5	36.840	416.5	1874	616.9	1644	878.0	925.3	1280	416.7	1682	198.6	2084	98.0	2486	49.72	8450	0.480
216.5	32.890	417.5	1693	617.9	1700	880.0	926.3	1282	373.2	1684	207.8	2086	99.5	2488	51.24	8500	0.469
217.5	35.960	418.5	1713	618.9	1699	882.0	914.5	1284	408.6	1686	208.6	2088	99.1	2490	51.23	8550	0.459
218.5	45.220	419.5	1730	619.9	1715	884.0	928.3	1286	413.1	1688	208.3	2090	98.9	2492	51.06	8600	0.448
219.5	47.820	420.5	1788	620.9	1727	886.0	913.5	1288	413.7	1690	206.4	2092	95.6	2494	50.48	8650	0.438
220.5	48.240	421.5	1828	621.9	1698	888.0	915.4	1290	409.5	1692	209.8	2094	96.5	2496	50.64	8700	0.429
221.5	40.330	422.5	1609	622.9	1697	890.0	911.5	1292	412.3	1694	208.4	2096	96.1	2498	50.45	8750	0.419
222.5	50.600	423.5	1740	624.8	1664	892.0	902.6	1294	409.3	1696	207.7	2098	96.8	2500	50.61	8800	0.410
223.5	64.220	424.5	1798	625.8	1662	894.0	905.5	1296	411.4	1698	206.8	2100	96.7	2520	49.22	8850	0.401
224.5	60.100	425.5	1724	626.8	1709	896.0	910.5	1298	406.5	1700	203.4	2102	96.3	2540	47.82	8900	0.393
225.5	53.290	426.5	1727	627.8	1715	898.0	885.7	1300	408.3	1702	201.8	2104	96.4	2560	46.46	8950	0.384
226.5	40.160	427.5	1596	628.8	1712	900.0	880.8	1302	403.2	1704	202.1	2106	96.4	2580	45.15	9000	0.376
227.5	40.690	428.5	1614	629.8	1685	902.0	882.7	1304	400.4	1706	202.4	2108	95.9	2600	43.89	9050	0.368

228.5	52.940	429.5	1501	630.7	1682	904.0	872.8	1306	403.4	1708	199.0	2110	94.0	2620	42.68	9100	0.360
229.5	48.620	430.5	1155	631.7	1649	906.0	872.8	1308	401.6	1710	200.3	2112	95.1	2640	41.50	9150	0.353
230.5	53.120	431.5	1715	632.7	1684	908.0	846.1	1310	399.9	1712	192.3	2114	94.7	2660	40.37	9200	0.345
231.5	51.950	432.5	1674	633.7	1662	910.0	857.0	1312	390.1	1714	201.0	2116	92.9	2680	39.28	9250	0.338
232.5	54.280	433.5	1760	634.7	1673	912.0	864.9	1314	397.3	1716	198.7	2118	93.9	2700	38.22	9300	0.331
233.5	45.600	434.5	1698	635.7	1668	914.0	857.0	1316	384.9	1718	198.0	2120	92.8	2720	37.20	9350	0.324
234.5	39.710	435.5	1752	636.6	1663	916.0	852.0	1318	393.1	1720	195.0	2122	93.0	2740	36.21	9400	0.318
235.5	52.400	436.5	1962	637.6	1688	918.0	853.0	1320	394.2	1722	194.8	2124	91.5	2760	35.26	9450	0.311
236.5	49.520	437.5	1837	638.6	1682	920.0	827.3	1322	391.2	1724	188.4	2126	92.0	2780	34.34	9500	0.305
237.5	49.370	438.5	1594	639.6	1645	922.0	820.3	1324	391.6	1726	192.4	2128	92.6	2800	33.45	9550	0.299
238.5	42.770	439.5	1857	640.6	1633	924.0	826.3	1326	388.0	1728	191.5	2130	92.0	2820	32.59	9600	0.293
239.5	44.970	440.5	1742	641.5	1626	926.0	831.2	1328	386.8	1730	192.5	2132	92.1	2840	31.75	9650	0.287
240.5	40.310	441.5	1964	642.5	1642	928.0	837.2	1330	379.1	1732	188.7	2134	91.7	2860	30.95	9700	0.281
241.5	52.460	442.5	2014	643.5	1635	930.0	832.2	1332	379.5	1734	179.2	2136	89.6	2880	30.17	9750	0.276
242.5	71.960	443.5	1942	644.5	1637	932.0	840.1	1334	385.9	1736	174.6	2138	91.2	2900	29.41	9800	0.270
243.5	67.810	444.5	2007	645.5	1621	934.0	827.3	1336	382.9	1738	180.7	2140	90.6	2920	28.68	9850	0.265
244.5	62.140	445.5	1853	646.4	1622	936.0	812.4	1338	380.5	1740	185.6	2142	90.5	2940	27.97	9900	0.260
245.5	50.340	446.5	1924	647.4	1633	938.0	820.3	1340	375.4	1742	183.9	2144	89.8	2960	27.28	9950	0.255
246.5	51.370	447.5	2112	648.4	1634	940.0	813.4	1342	378.5	1744	186.9	2146	89.0	2980	26.62	10 000	0.250
247.5	56.570	448.5	2007	649.4	1570	942.0	798.5	1344	378.5	1746	183.0	2148	89.6	3000	25.97	11 000	0.170
248.5	46.530	449.5	2062	650.3	1630	944.0	814.4	1346	375.7	1748	182.2	2150	89.2	3020	25.35	12 000	0.119
249.5	57.460	450.5	2180	651.3	1645	946.0	809.4	1348	376.4	1750	182.7	2152	88.5	3040	24.74	13 000	8.65E − 2
250.5	61.250	451.5	2145	652.3	1618	948.0	793.6	1350	370.2	1752	181.7	2154	88.3	3060	24.15	14 000	6.42E − 2
251.5	46.890	452.5	1974	653.3	1605	950.0	795.6	1352	373.4	1754	183.7	2156	88.1	3080	23.58	15 000	4.86E − 2
252.5	42.340	453.5	2004	654.3	1589	952.0	788.6	1354	371.8	1756	182.8	2158	87.8	3100	23.03	16 000	3.75E − 2
253.5	52.540	454.5	2013	655.2	1537	954.0	777.7	1356	361.6	1758	182.4	2160	87.0	3120	22.49	17 000	2.93E − 2
254.5	60.710	455.5	2069	656.2	1303	956.0	791.6	1358	368.6	1760	181.8	2162	86.0	3140	21.97	18 000	2.33E − 2
255.5	80.820	456.5	2112	657.2	1456	958.0	788.6	1360	363.4	1762	176.6	2164	84.2	3160	21.47	19 000	1.87E − 2
256.5	103.800	457.5	2136	658.2	1567	960.0	784.7	1362	365.9	1764	179.4	2166	75.6	3180	20.98	20 000	1.52E − 2
257.5	127.800	458.5	2005	659.1	1563	962.0	779.3	1364	361.3	1766	180.5	2168	82.6	3200	20.50	25 000	6.28E − 3
258.5	127.500	459.5	2043	660.1	1580	964.0	777.2	1366	364.0	1768	178.5	2170	84.7	3220	20.04	30 000	3.04E − 3

(*continued overleaf*)

Table 16.3 (*continued*)

λ [nm]	$E(\lambda)$ [Wm^{-2} μm^{-1}]	λ [nm]	$E(\lambda)$ [Wm^{-2} μm^{-1}]	λ [nm]	$E(\lambda)$ [Wm^{-2} μm^{-1}]	λ [nm]	$E(\lambda)$ [Wm^{-2} μm^{-1}]	λ [nm]	$E(\lambda)$ [Wm^{-2} μm^{-1}]	λ [nm]	$E(\lambda)$ [Wm^{-2} μm^{-1}]	λ [nm]	$E(\lambda)$ [Wm^{-2} μm^{-1}]	λ [nm]	$E(\lambda)$ [Wm^{-2} μm^{-1}]	λ [nm]	$E(\lambda)$ [Wm^{-2} μm^{-1}]
259.5	106.000	460.5	2075	661.1	1585	966.0	767.2	1368	358.4	1770	177.1	2172	85.0	3240	19.59	35 000	1.64E − 3
260.5	87.150	461.5	2090	662.0	1597	968.0	771.7	1370	356.4	1772	177.8	2174	85.1	3260	19.15	40 000	9.65E − 4
261.5	91.520	462.5	2140	663.0	1569	970.0	767.5	1372	359.3	1774	177.7	2176	84.1	3280	18.72	50 000	3.97E − 4
262.5	105.600	463.5	2075	664.0	1558	972.0	771.9	1374	357.4	1776	174.3	2178	82.7	3300	18.31	60 000	1.92E − 4
263.5	168.900	464.5	2010	665.0	1575	974.0	754.1	1376	352.6	1778	173.0	2180	84.8	3320	17.91	80 000	6.10E − 5
264.5	254.500	465.5	2077	665.9	1567	976.0	760.4	1378	356.3	1780	173.3	2182	82.9	3340	17.52	1 00 000	2.51E − 5
265.5	257.500	466.5	1954	666.9	1555	978.0	756.1	1380	355.6	1782	172.7	2184	84.1	3360	17.14	1 20 000	1.21E − 5
266.5	254.200	467.5	2049	667.9	1554	980.0	752.4	1382	351.4	1784	172.5	2186	84.0	3380	16.77	1 50 000	4.98E − 6
267.5	255.600	468.5	2028	668.8	1569	982.0	755.1	1384	353.8	1786	171.5	2188	81.2	3400	16.41	2 00 000	1.58E − 6
268.5	248.500	469.5	2024	669.8	1554	984.0	749.2	1386	349.4	1788	173.4	2190	82.7	3420	16.06	2 50 000	6.51E − 7
269.5	243.500	470.5	1909	670.8	1551	986.0	745.6	1388	351.5	1790	171.7	2192	83.2	3440	15.72	3 00 000	3.06E − 7
270.5	272.400	471.5	2052	671.8	1541	988.0	742.9	1390	348.1	1792	170.4	2194	82.8	3460	15.39	4 00 000	1.05E − 7
271.5	228.700	472.5	2076	672.7	1537	990.0	732.0	1392	349.3	1794	168.9	2196	82.5	3480	15.07	10 00 000	3.51E − 9
272.5	201.200	473.5	2025	673.7	1533	992.0	738.7	1394	347.0	1796	168.8	2198	82.5	3500	14.76	10 00 000	3.51E − 9
273.5	200.200	474.5	2086	674.7	1530	994.0	737.6	1396	345.3	1798	168.5	2200	82.1	3520	14.45	–	–
274.5	135.200	475.5	2050	675.6	1527	996.0	733.6	1398	346.8	1800	167.6	2202	81.6	3540	14.16	–	–
275.5	178.500	476.5	1990	676.6	1523	998.0	731.4	1400	339.2	1802	164.5	2204	81.7	3560	13.87	–	–
276.5	247.500	477.5	2110	677.6	1520	1000.0	728.0	1402	340.3	1804	166.6	2206	77.4	3580	13.58	–	–
277.5	238.200	478.5	2043	678.5	1518	1002.0	725.8	1404	338.1	1806	165.5	2208	79.3	3600	13.31	–	–
278.5	162.300	479.5	2111	679.5	1515	1004.0	709.7	1406	337.9	1808	165.3	2210	80.6	3620	13.04	–	–
279.5	87.190	480.5	2070	680.5	1513	1006.0	685.9	1408	338.5	1810	164.9	2212	80.5	3640	12.78	–	–
280.5	96.450	481.5	2126	681.4	1510	1008.0	714.5	1410	338.2	1812	163.1	2214	80.2	3660	12.53	–	–
281.5	212.300	482.5	2058	682.4	1508	1010.0	713.4	1412	329.6	1814	161.3	2216	79.2	3680	12.28	–	–
282.5	299.800	483.5	2053	683.4	1506	1012.0	709.5	1414	330.7	1816	156.9	2218	79.2	3700	12.04	–	–
283.5	319.500	484.5	2003	684.3	1504	1014.0	702.9	1416	333.3	1818	145.6	2220	79.5	3720	11.80	–	–
284.5	239.800	485.5	1862	685.3	1503	1016.0	697.1	1418	332.9	1820	155.8	2222	79.1	3740	11.57	–	–
285.5	166.300	486.5	1653	686.3	1501	1018.0	694.6	1420	329.7	1822	154.6	2224	78.8	3760	11.35	–	–
286.5	328.900	487.5	1862	687.2	1500	1020.0	691.0	1422	321.9	1824	159.4	2226	77.1	3780	11.13	–	–
287.5	342.800	488.5	1947	688.2	1499	1022.0	687.5	1424	325.9	1826	159.3	2228	78.0	3800	10.92	–	–

288.5	328.400	489.5	1994	689.1	1506	1024.0	694.0	1426	320.2	1828	157.1	2230	77.9	3820	10.71	–	–
289.5	481.800	490.5	2041	690.1	1512	1026.0	691.4	1428	319.5	1830	158.5	2232	77.9	3840	10.50	–	–
290.5	612.800	491.5	1929	691.1	1506	1028.0	690.5	1430	321.0	1832	157.0	2234	77.8	3860	10.31	–	–
291.5	592.000	492.5	1929	692.0	1495	1030.0	680.2	1432	322.4	1834	156.1	2236	77.3	3880	10.11	–	–
292.5	531.900	493.5	1921	693.0	1495	1032.0	682.3	1434	321.5	1836	156.1	2238	75.7	3900	9.92	–	–
293.5	545.800	494.5	2093	694.0	1498	1034.0	664.4	1436	322.5	1838	154.0	2240	76.2	3920	9.74	–	–
294.5	518.500	495.5	1959	694.9	1480	1036.0	675.4	1438	323.1	1840	154.3	2242	76.1	3940	9.56	–	–
295.5	563.800	496.5	2051	695.9	1489	1038.0	665.5	1440	308.8	1842	151.3	2244	76.2	3960	9.38	–	–
296.5	519.400	497.5	2052	696.8	1489	1040.0	664.4	1442	314.5	1844	152.5	2246	76.1	3980	9.21	–	–
297.5	517.000	498.5	1898	697.8	1457	1042.0	664.3	1444	311.6	1846	153.5	2248	74.7	4000	9.04	–	–
298.5	474.400	499.5	2004	698.8	1494	1044.0	666.3	1446	317.4	1848	147.2	2250	75.5	4020	8.87	–	–
299.5	493.300	500.5	1889	699.7	1486	1046.0	651.0	1448	314.7	1850	153.0	2252	75.0	4040	8.69	–	–
300.5	428.000	501.5	1843	700.7	1462	1048.0	655.3	1450	312.2	1852	151.8	2254	73.7	4060	8.52	–	–
301.5	464.300	502.5	1927	701.6	1455	1050.0	656.5	1452	308.0	1854	150.5	2256	74.2	4080	8.35	–	–
302.5	498.300	503.5	1967	702.6	1462	1052.0	653.4	1454	307.9	1856	148.0	2258	74.5	4100	8.18	–	–
303.5	632.500	504.5	1901	703.6	1468	1054.0	647.3	1456	306.6	1858	149.8	2260	74.3	4120	8.02	–	–
304.5	614.000	505.5	2027	704.5	1482	1056.0	650.1	1458	311.8	1860	147.2	2262	72.6	4140	7.87	–	–
305.5	606.200	506.5	1995	705.5	1472	1058.0	633.3	1460	309.6	1862	146.0	2264	73.5	4160	7.71	–	–
306.5	566.400	507.5	1939	706.4	1452	1060.0	634.8	1462	306.0	1864	146.6	2266	72.9	4180	7.56	–	–
307.5	626.800	508.5	1952	707.4	1455	1062.0	640.7	1464	305.5	1866	144.1	2268	73.2	4200	7.42	–	–
308.5	623.200	509.5	1949	708.3	1442	1064.0	633.8	1466	303.7	1868	144.1	2270	73.1	4220	7.27	–	–
309.5	506.000	510.5	1980	709.3	1426	1066.0	627.2	1468	304.5	1870	145.4	2272	72.6	4240	7.13	–	–
310.5	634.300	511.5	2031	710.3	1440	1068.0	621.4	1470	302.3	1872	140.7	2274	72.1	4260	7.00	–	–
311.5	743.200	512.5	1899	711.2	1416	1070.0	611.3	1472	300.6	1874	136.6	2276	72.5	4280	6.86	–	–
312.5	668.500	513.5	1893	712.2	1408	1072.0	620.4	1474	295.8	1876	119.0	2278	72.3	4300	6.74	–	–
313.5	713.300	514.5	1906	713.1	1408	1074.0	611.3	1476	296.4	1878	139.0	2280	71.9	4320	6.61	–	–
314.5	675.600	515.5	1933	714.1	1413	1076.0	610.6	1478	294.1	1880	140.3	2282	68.8	4340	6.48	–	–
315.5	645.100	516.5	1697	715.0	1398	1078.0	606.6	1480	300.0	1882	142.1	2284	71.1	4360	6.36	–	–
316.5	645.300	517.5	1755	716.0	1403	1080.0	616.9	1482	297.5	1884	141.3	2286	70.8	4380	6.25	–	–
317.5	788.800	518.5	1682	716.9	1407	1082.0	588.3	1484	293.2	1886	138.5	2288	71.0	4400	6.13	–	–
318.5	677.600	519.5	1860	717.9	1400	1084.0	596.4	1486	296.0	1888	141.4	2290	70.8	4420	6.02	–	–
319.5	724.100	520.5	1863	718.8	1376	1086.0	607.3	1488	273.1	1890	137.6	2292	70.5	4440	5.91	–	–

technologies and as long as methods for the correlation between results using the reference spectrum and results from "real world" spectra is established. The technical basis for the direct spectra has recently been reexamined and found to have a diffuse component that is substantially greater than that concentrators would normally encounter [19, 20]. On examination of the US solar radiation database, it was found that when the global-normal irradiance is near 1000 Wm^{-2}, the direct-normal component is near 850 Wm^{-2} and not the 767 Wm^{-2} that the direct standard spectrum integrates into [20]. This difference has been attributed to an aerosol optical depth at 500 nm of 0.27 in the terrestrial reference spectra [20]. This has not been a problem for single junction PV concentrators in the past because of their relative insensitivity to the specific direct spectra [21]. Recent high-efficiency structures such as the GaInP/GaAs/Ge triple-junction solar cell exhibit a significant difference in the efficiency between the global and direct reference spectrum (>10% relative) [22, 23] as shown in Figure 16.2. It has been proposed that the direct reference spectrum be modified to have a lower aerosol optical depth of 0.066 broadband or 0.085 at 500 nm to better represent the spectral irradiance in sunny regions (average daily direct-beam energy greater than 6 $\mathrm{kWh/m^2/day}$) where concentrators might be deployed [22]. This low aerosol optical depth direct beam reference spectrum was generated using the same atmospheric conditions as the current terrestrial reference spectrum [10, 12, 13, 18] and has been adopted at NREL for evaluating concentrators as of January 2003. Tabular values of this direct beam spectrum can be found at the following web sites: *http://www.nrel.gov/highperformancepv/* or *http://rredc.nrel.gov/solar/standards/am1.5/*.

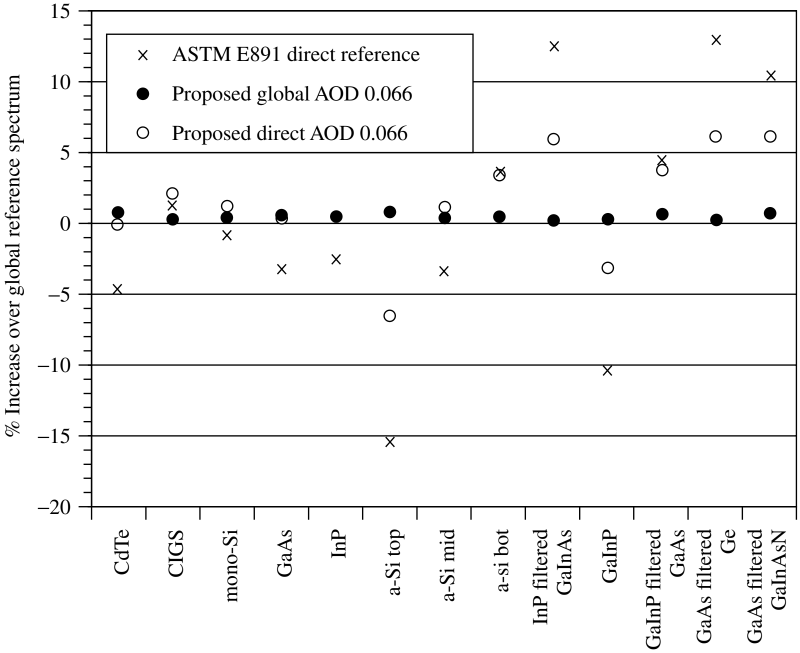

Figure 16.2 Percentage change in the normalized short-circuit current from the normalized global reference spectrum for various state-of-the-art PV technologies compared with the proposed direct reference spectra

The extraterrestrial spectral irradiance distribution at one astronomical unit distance from the sun is commonly referred to as the AM0 spectrum. At present, international consensus standards do not exist for AM0 measurements. Each country's space agency has adopted its own internal procedures. However, an international standard is in the draft stage [15]. Measurements of the total AM0 irradiance used by the aerospace community have varied from 1353 $\mathrm{Wm^{-2}}$ to 1372 $\mathrm{Wm^{-2}}$ [8, 14, 16, 24, 25]. Many groups still rely on the less accurate value of 1353 $\mathrm{Wm^{-2}}$ total AM0 irradiance [16, 24]. Recently, a new ASTM AM0 standard has been adopted that uses more accurate spectral irradiance measurements that are given in Table 16.3 and Figure 16.1 [8]. The best estimate for the solar "constant" is 1367 $\mathrm{Wm^{-2}}$ recommended by the World Radiation Center [14] or 1366.1 recommended by ASTM [8]. Both of these values were obtained from long-term monitoring of the solar irradiance with an active-cavity radiometer on the Solar Max and Nimbus 7 and other satellites [26]. Fortunately, the 1353 $\mathrm{Wm^{-2}}$ total AM0 irradiance, used by many groups for efficiency measurements and reporting purposes does not enter into the spacecraft PV power measurements. This is because primary balloon or space-based AM0 reference cells are calibrated at whatever irradiance that exists at the time of calibration, corrected to one astronomical unit distance from the sun. This means that numerical values of the AM0 total irradiance and spectral irradiance are not used in calibrating primary AM0 reference cells as discussed in Section 16.3.3.

A variety of definitions for cells and modules have been proposed [1, 5, 27, 28]. A module consists of several encapsulated, environmentally protected, and electrically interconnected cells. The area of a cell is taken to be the total area of the space charge region which includes grids and contacts. The standard cell area definitions replace the term *space charge region* with frontal area, but this term does not adequately account for devices with multiple cells on a single substrate or superstrate. The area of a concentrator cell is based upon the cell area that is designed to be illuminated [5]. This area is taken to be the area of the space charge region minus the area of any peripheral bus bars or contacts. A submodule or minimodule is an unencapsulated module.

The PV efficiency (η) is inversely proportional to the area definition used (equation 16.1). In fact, differences in the area definition often account for the greatest differences in η between various groups and values published in the literature [28, 29]. The largest differences occur when the so-called active area (total device area minus all area that is shaded or not active) is used. The use of an active area in the efficiency neglects the trade-off between lower resistance losses and increased shading. Several thin-film PV device structures do not have any shading losses, so the active and total area is the same. To prevent an artificial increase in the efficiency, care must be taken to ensure that light outside the defined area cannot be collected by multiple internal reflections or that carriers generated outside the defined area are collected due to incomplete electrical isolation. The smaller the cell area, the larger this possible effect. The larger the perimeter-to-area ratio, the greater the effect of the current being collected outside the defined area. This phenomenon is the reason a 1-$\mathrm{cm^2}$ minimum area is required for inclusion in the *Progress in Photovoltaics* efficiency tables [30]. To be sure that the region enclosed by the total area is the only active region, an aperture should be used [30]. At the module level, the total area including the frame is used. For prototype modules, where the frame design is less important than the encapsulation and cell interconnections, an aperture-area definition is often used. The aperture-area definition is the total area minus the frame area.

This aperture area may be defined by opaque tape if there is no frame to eliminate the possibility of the module collecting current outside the defined aperture area by multiple internal reflections or light piping.

The most common performance rating method for modules is the PV power conversion efficiency under SRC (Table 16.1). The power or peak watt rating on the module's nameplate is usually given with respect to SRC, as shown in Table 16.1 using a 25°C module temperature. Unfortunately, prevailing conditions under natural sunlight do not commonly match nameplate conditions. The nameplate rating that the manufacturer assigns to a given module model number is often higher than the measured power output in the field [31–33]. If the nameplate rating is determined at 25°C, then the actual power produced is often less than this because the module will typically run at 40° to 60°C. The temperature coefficient for the peak power is usually negative. The nameplate rating also does not include long-term degradation or system losses. System losses include the power-conditioning unit's efficiency, ability of the power conditioner to operate at the maximum PV power point, orientation, shading, resistance losses in the wiring, and mismatch in the power of different modules.

The nominal operating cell temperature (NOCT) is a rating designed to give information about the thermal qualities of a module and a more realistic estimate of the power in the field on a sunny day at solar noon. The NOCT of a module is a fixed temperature that the module would operate at if it is exposed to the nominal thermal environment (20°C air temperature, 800 Wm^{-2} total irradiance, and a wind speed of 1 ms^{-1}) [7, 34]. The term "standard operating conditions" or SOC is sometimes used for flat-plate or concentrator-terrestrial modules operating at NOCT. The actual determination of the NOCT of a module with an uncertainty of less than ±2°C has proved difficult because of difficulties in measuring the temperature of cells in an encapsulated module, uncertainties in the total irradiance, and secondary environmental effects such as wind direction, ground reflections, mounting, and electrical loading [34, 35]. The installed NOCT is up to 15°C warmer for roof-mounted applications than a free-standing module depending on the stand off distance between the module and the roof [34, 35]. The module temperature can be calculated from the NOCT or installed NOCT and air temperature using

$$T = T_{\mathrm{air}} + (\mathrm{NOCT} - 20^{\circ}\mathrm{C})E_{\mathrm{tot}}/800\ \mathrm{Wm}^{-2}. \tag{16.2}$$

A wind speed correction can also be applied to equation (16.2) [7, 34].

For a fair and meaningful comparison of efficiencies between technologies, the measurements should be performed after any initial degradation. Commercial silicon modules have shown small changes in performance after the first few hours of operation [36, 37]. At the present time, all amorphous silicon PV technologies degrade when exposed to sunlight. Fortunately, this degradation stabilizes at a level of 80% to 90% of the initial value (see Chapter 12). Partial recovery occurs in the field during the summer when the higher module temperature leads to partial annealing or when amorphous silicon modules are annealed in the laboratory at 60° to 70°C [38, 39]. The efficiency continues to decrease after 500 h of light exposure at lower temperatures even if the light level is reduced [38–40]. For a fair and meaningful comparison of improvements in amorphous silicon module development, the performance at SRC is now reported after illumination of about 1000 Wm^{-2}, at a module back-surface temperature of nominally 50°C, for at least 1000 h, with a resistive load near $P_{\max}$, and low humidity [28, 39]. These conditions were chosen to approximate one year of outdoor exposure without the humidity or temperature cycling. Other thin-film module technologies may undergo reversible and irreversible changes during the first few hours of light exposure [29, 41, 42].

16.2.2 Alternative Peak Power Ratings

A variety of groups have suggested and adopted alternative rating schemes to compare module and system performance between the various PV technologies. These schemes are based on measurements of a module's performance in the field and on performing a regression analysis on the data. The site-specific power production is more relevant for bulk power generation than the power with respect to a particular theoretical reference spectrum and module operating temperature.

One popular method was adopted by Pacific Gas and Electric Company and the Photovoltaics for Utility-Scale Applications (PVUSA) project in California, USA, to rate and purchase PV systems. They perform a linear regression analysis on the actual measured system or module power produced (P), air temperature (T_a), wind speed (S), and total plane-of-array irradiance (E_{tot}) as measured with a pyranometer or radiometer:

$$P = P_{\max}(E_{\text{tot}}, T_a, S) = E_{\text{tot}}(C_1 + C_2 E_{\text{tot}} + C_3 T_a + C_4 S), \tag{16.3}$$

where C_1, C_2, C_3, and C_4 are the regression coefficients [32, 43]. The goal of performing a multiple regression analysis on the measured power to a fixed set of environmental conditions is to accurately represent the average power output under clear-sky conditions near midday at a given site. The power can be measured at the maximum direct-current (DC) power point, or on the DC side of the inverter, or at the alternating-current (AC) power out of the inverter. The last two power measurement locations will include some system losses. This site-specific rating scheme takes into account the different thermal characteristics of modules and spectral sensitivities since it is not referenced to a standard spectrum or module temperature. The power rating is evaluated using equation (16.3) at $T_a = 20°\text{C}$, $S = 1\ \text{ms}^{-1}$, and $E_{\text{tot}} = 1000\ \text{Wm}^{-2}$ for flat-plate collectors. For concentrators, the direct-normal incidence sunlight within a 5° or 5.7° field of view of 850 Wm^{-2} is used for E_{tot}. The difference between the fields of view is because an absolute-cavity radiometer has a 5° field of view and some less accurate but less expensive normal incidence pyrheliometers have a 5.7° field of view.

The primary advantage of basing the reference temperature on the air temperature is that the different thermal characteristics of the module, array, and system are included in the rating, and the power rating is closer to what is actually observed. The different spectral conditions at the different sites are also accounted for by not referencing the performance to a fixed spectrum, but rather, referencing the power to the actual spectrum that was incident on the module. If a PV reference cell is used to measure E_{tot}, then the power would be with respect to a reference spectrum at all light levels. Spectral mismatch issues associated with E_{tot}, measured with a thermal- or spectrally matched detector are discussed further in Section 16.3.1.

16.2.3 Energy-based Performance Rating Methods

Despite its widespread acceptance, the peak power rating (i.e. maximum instantaneous watts) does not capture the differences among the plethora of flat-plate and concentrator-module designs with different total irradiance, diffuse irradiance, spectral irradiance, and temperature sensitivities. Energy-based ratings (i.e. integrated power over time in kWh) capture the module performance in the "real" world. It is easy to integrate the measured PV power produced over a time interval to obtain the total energy produced compared with the incident energy. A variety of rating criteria besides the standard reference conditions listed in Table 16.1 exist, depending on the application in Table 16.4.

The AM/PM method, proposed by ARCO/Siemens Solar Industries, attempts to rate a module in terms of the PV energy produced during a standard solar day with a given reference temperature and total irradiance distribution [44]. The AM/PM method is appealing because it is an energy-rating method that is not site-specific. A variation on the AM/PM energy-rating method was developed in which a regression analysis of the measured power and irradiance data to a nonlinear response function was summed over a standard day defined by a fourth-order polynomial [45].

A rating scheme based on the PV energy delivered over a standard day has been proposed for a small set of standard days [46–49]. These five days were obtained from the typical meteorological year database (*http://rredc.nrel.gov/solar/old_data/*) corresponding to a hot-sunny, cold-sunny, hot-cloudy, cold-cloudy, and a nice day [49, 50]. The meteorological data for the standard days include latitude, longitude, date, air temperature, wind speed, relative humidity, and direct, diffuse-horizontal, and global-normal irradiances. The direct-beam and plane-of-array spectral irradiances were then computed for hourly intervals throughout the day using a spectral model [51]. The model developed by Nann requires only the meteorological parameters listed in the standard days. Figure 16.3 shows the meteorological characteristics of the hot-sunny standard day [46–49]. The hot-sunny day was taken from the meteorological data for Phoenix Arizona, US, on June 24, 1976 [49, 50].

Other schemes for energy rating based on site-specific conditions instead of standard days have also been developed. In 1990, a rating based on realistic reporting conditions (RRC) was proposed. This method measured the performance of PV modules under different irradiances and temperatures and predicted the module's output under

Table 16.4 Photovoltaic rating criterion for PV applications

Application	Relevant PV parameter
Grid-connected, hydrogen production	Annual energy delivered
Power for peak utility demand	Power near solar noon
Remote system for cooling	Temperature coefficient and NOCT
Remote system with storage	Energy during cloudy day
Pump system for agriculture	Energy during growing season
Small power consumer products	Efficiency at very low irradiance
High value (Space)	High efficiency, radiation, and thermal stability

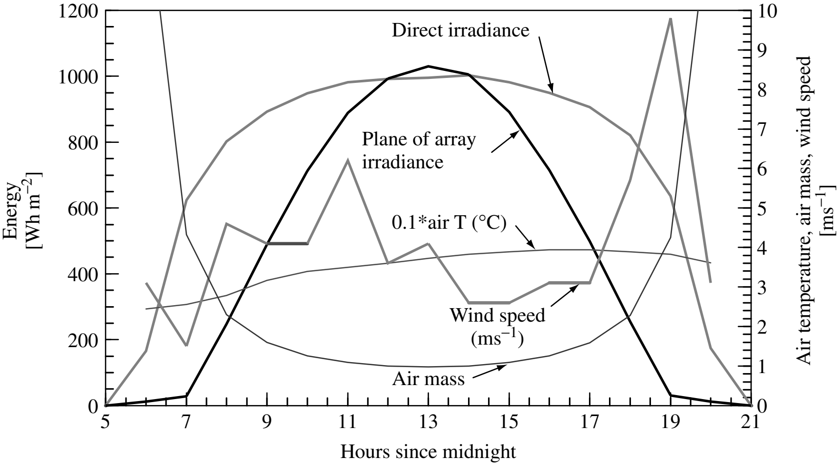

Figure 16.3 Meteorological conditions for the hot-sunny reference day [46–49]

various operating conditions [3, 4, 52–54]. This method has been used to compare commercial modules, highlighting the different dependencies on light level and temperature. Figure 16.4 illustrates the comparative ratings of selected modules for various locations in the United States [52] and Europe [53]. The results in Figure 16.4 indicate that the annual PV efficiency is 2 to 20% less than the efficiency under SRC (25°C, 1000 Wm^{-2}, and the global reference spectrum). The annual PV efficiency is total PV energy divided by the total energy deposited on a south-facing surface tilted to the latitude of the site. Spectral effects were ignored in Figure 16.4 with the global reference spectrum in Table 16.2 used for all calculations, so only temperature and total irradiance effects are included. The solar cell was modeled as described in Chapter 3 with a double exponential with series resistance and shunt resistance to model the performance as a function of total irradiance and temperature. Current state-of-the-art modules may be less sensitive to temperature and irradiance variations because of smaller temperature coefficients, series resistance, dark current, and a larger shunt resistance. The deviation of the annual efficiency from the efficiency under SRC would have been less if two-axis tracking were assumed. However, most flat-plate systems do not employ two-axis tracking. The spectral model developed by Nann was coupled with a PV model to compare the performance of a variety of PV technologies [4]. The PV model used a double exponential with series and shunt resistances to fit to the highest-efficiency cells made at the time of each technology. The environmental conditions include time, date, global-horizontal irradiance, direct-normal irradiance, diffuse irradiance, plane-of-array irradiance, ambient temperature, wind speed, and relative humidity. The results of the study were similar to those summarized in Figure 16.4 and References [52, 53]. The spectral model confirmed that the spectral sensitivity of Si, CdTe, $CuInSe_2$, and GaAs technologies on the annual energy production is +1% to −3%. The results also show that the efficiency of single- and multijunction amorphous silicon is ~10% less in winter months solely from spectral effects [4].

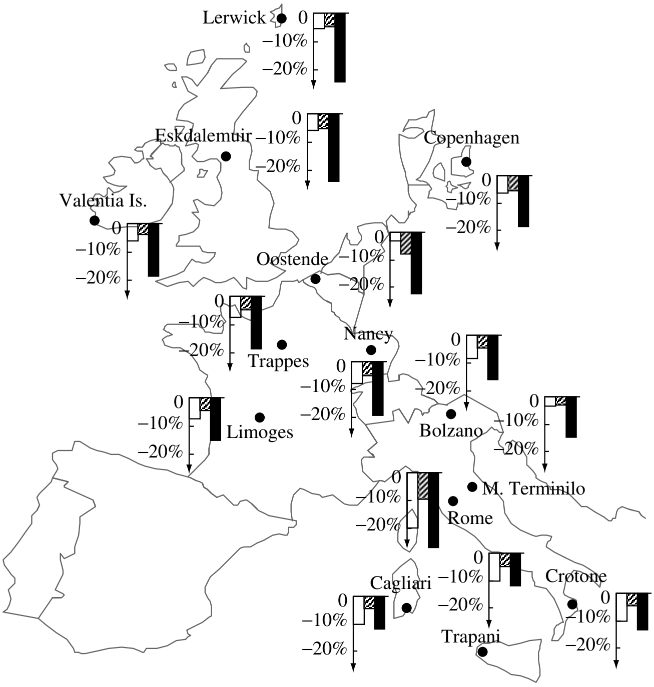

(a)

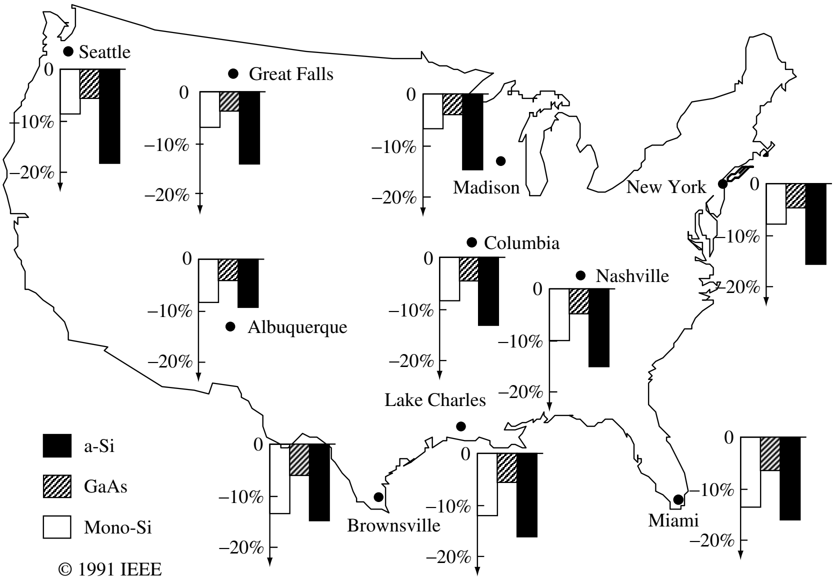

© 1991 IEEE

(b)

Figure 16.4 Example of PV performance on a yearly basis normalized to standard reference conditions for three different solar cell technologies (a-Si, GaAs, and c-Si) showing the percentage of deviation from standard conditions for a variety of locations in (a) Europe [52] and (b) the United States [53]

16.2.4 Translation Equations to Reference Conditions

The most basic translation equations for a solar cell are based on the diode model with series and shunt resistances discussed in Chapters 3 and 7. This model has been extended to modules by combining them in series and parallel combinations [55].

To a first order, short-circuit current (I_{SC}), open-circuit voltage (V_{OC}), P_{max}, and fill factor (FF) are linear with temperature, whereas the current is linear with E_{tot} [49, 56–60]. These linear translation equations allow the performance under standard reference conditions to be translated to other conditions for energy-based rating methods. Typical temperature coefficients for various PV technologies are summarized in Table 16.5 and Figure 16.5.

A set of translation equations for current and voltage based on the work of Sandstrom has been implemented in consensus standards [61, 62]. These equations translate the entire current versus voltage ($I-V$) curve for temperature and irradiance. Following the notation of the international standard in Reference [62], the following equations allow one to translate the current I_1 and voltage V_1 measured from temperature T_1 to T_2 and irradiance E_1 to E_2:

$$I_2 = I_1 + I_{SC1}\left(\frac{E_2}{E_1} - 1\right) + \alpha(T_2 - T_1) \tag{16.4}$$

$$V_2 = V_1 - R_s(I_2 - I_1) - I_2K(T_2 - T_1) + \beta(T_2 - T_1), \tag{16.5}$$

where α and β are the temperature coefficients, R_s is the series resistance, and K is a curve-shape correction factor. Applying equations (16.4) and (16.5) at a fixed irradiance

Table 16.5 Typical Si solar cell temperature coefficients [57]

Type	$-V_{OC}$ [ppm/°C]	I_{SC} [ppm/°C]	$-FF$ [ppm/°C]	$-P_{max}$ [ppm/°C]
Si cells & modules	2400–4500	400–980	940–1700	2600–5500

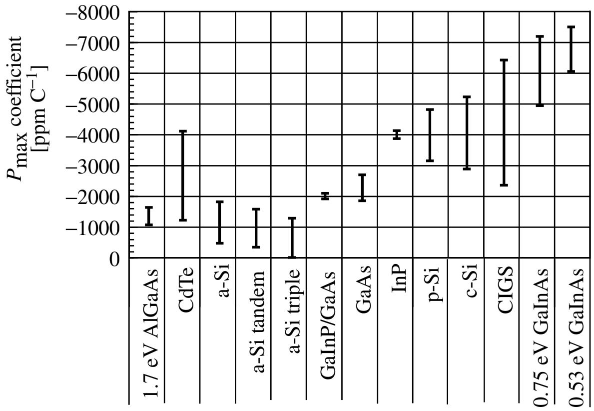

Figure 16.5 Typical P_{max} temperature coefficients of various PV technologies [57]

($E_2 = E_1$) and assuming no series resistance ($R_s = 0$), the value of K that best translates the $I-V$ characteristics for temperature is determined.

Translation equations for I_{SC}, V_{OC}, V_{max}, and I_{max} as a function of E_{tot}, T_c, absolute air mass (AM_a), and angle of incidence (AOI) based on multiple regression analysis of field data have been proposed by King [63]:

$$I_{SC}(E, T_c, AM_a, AOI) = (E/E_0) f_1(AM_a) f_2(AOI)[I_{SC0} + \alpha_{I_{SC}}(T_c - T_o)] \tag{16.6}$$

$$E_e = I_{SC}(E, T_c = T_0, AM_a, AOI)/I_{SC0} \tag{16.7}$$

$$I_{mp}(E_e, T_c) = C_0 + E_{ec}[C_1 + \alpha_{I_{mp}}(T_c - T_0)] \tag{16.8}$$

$$V_{OC}(E_e, \mathrm{i}) = V_{OC0} + C_2 \ln(E_e) + \beta_{V_{OC}}(T_c - T_0) \tag{16.9}$$

$$V_{mp}(E_e, T_c) = V_{mp0} + C_3 \ln(E_e) + C_4[\ln(E_e)]^2 + \beta_{V_{mp}}(T_c - T_0) \tag{16.10}$$

$$I_{SC0} = I_{SC}(E = E_0, T_c = T_0, AM_a = 1.5, AOI = 0^\circ) \tag{16.11}$$

$$V_{OC0} = V_{OC}(E_e = 1, T_c = T_0) \tag{16.12}$$

$$V_{mp0} = V_{mp}(E_e = 1, T_c = T_0) \tag{16.13}$$

$$f_2 = \frac{\dfrac{E_0}{I_{SC0}} I_{SC}(AM_a = 1.5, T_c = T_0) - E_{diff}}{E_{dir}\cos(\theta)}, \tag{16.14}$$

where E is the plane-of-array solar irradiance, E_e is the effective irradiance in units of suns, E_0 is the one-sun irradiance of 1000 Wm^{-2}, E_{diff} is the diffuse irradiance in the plane of the module, E_{dir} is the direct-normal irradiance, and AOI is the solar angle of incidence on the module; T_c is the temperature of the cells inside the module, T_0 is the module reference temperature, and $\alpha_{I_{SC}}$, α_{Imp}, $\beta_{V_{OC}}$, and $\beta_{V_{mp}}$ are the temperature coefficients of I_{SC}, I_{mp}, V_{OC}, and V_{mp}, respectively. These temperature coefficients are in absolute units so they will vary with the size of the PV device, the number of devices in series, or the number of devices in parallel. The pressure-corrected relative optical air mass AM_a can be written as [64]

$$AM_a = \frac{P}{P_0}[\cos(\theta) + 0.50572(96.07995^\circ - \theta)^{-1.6364}]^{-1}, \tag{16.15}$$

where P is the barometric pressure, P_0 is the pressure at sea level, and θ is the angle between the sun and zenith in degrees. The function $f_1(AM_a)$ is empirically obtained from the temperature- and irradiance-corrected I_{SC} versus air mass and assumes that the only spectral dependence is the zenith angle. Data are collected over a range of irradiances, incident angles, air masses, and temperatures and a multiple regression analysis is applied. These translation equations have been compared with simple linear translation equations derived from simulator-based measurements for several modules using outdoor data [49]. These translation equations give similar results to equation (16.3) when temperature, maximum-power tracking, and spectral issues are considered [48]. Other translation equations for current and voltage are possible [16, 65].